Carcinogenesis vol.30 no.3 pp.408–415, 2009
doi:10.1093/carcin/bgp004
Advance Access publication January 6, 2009

The DNA repair protein NBS1 influences the base excision repair pathway

Daniel Sagan[1,2,*], Romy Müller[1], Carina Kröger[1], Arunee Hematulin[1,2], Simone Mörtl[1] and Friederike Eckardt-Schupp[1]

[1]Institute of Radiation Biology, Helmholtz Centre Munich—German Research Centre for Environmental Health, Ingolstaedter Landstrasse 1, 85758 Neuherberg, Germany and [2]Department of Radiological Technology, Faculty of Allied Health Sciences, Naresuan University, Phitsanulok 65000, Thailand

[*]To whom correspondence should be addressed. Tel: +66 55 26 10 00 ext. 62 79; Fax: +66 55 26 19 35;
Email: daniel.sagan@helmholtz-muenchen.de

NBS1 fulfills important functions for the maintenance of genomic stability and cellular survival. Mutations in the *NBS1* (Nijmegen Breakage Syndrome 1) gene are responsible for the Nijmegen breakage syndrome (NBS) in humans. The symptoms of this disease and the phenotypes of *NBS1*-defective cells, especially their enhanced radiosensitivity, can be explained by an impaired DNA double-strand break-induced signaling and a disturbed repair of these DNA lesions. We now provide evidence that NBS1 is also important for cellular survival after oxidative or alkylating stress where it is required for the proper initiation of base excision repair (BER). *NBS1* downregulated cells show reduced activation of poly-(adenosine diphosphate-ribose)-polymerase-1 (PARP1) following genotoxic treatment with H_2O_2 or methyl methanesulfonate, indicating impaired processing of damaged bases by BER as PARP1 activity is stimulated by the single-strand breaks intermediately generated during this repair pathway. Furthermore, extracts of these cells have a decreased capacity for the *in vitro* repair of a double-stranded oligonucleotide containing either uracil or 8-oxo-7,8-dihydroguanine to trigger BER. Our data presented here highlight for the first time a functional role for *NBS1* in DNA maintenance by the BER pathway.

Introduction

Nijmegen breakage syndrome (NBS) is a recessive genetic disorder with immunodeficiency, growth retardation and a high frequency of malignancies as fundamental hallmarks (1,2). The *NBS1* gene affected in this disease encodes for the nuclear NBS1 protein (3,4), which forms a trimeric complex [MRE11/RAD50/NBS1 (MRN)] with its binding partners MRE11 and RAD50. The MRN complex is involved in DNA double-strand break (DSB)-signaling processes (5). The symptoms of NBS patients, as well as the phenotypes of NBS cells can be explained by a disturbed DSB-induced cell signaling, resulting in decreased genomic stability (1). Beside its well-known interaction partners MRE11 and RAD50, NBS1 interacts with the helicase WRN (6), which has been found to activate base excision repair (BER) by interacting with key components of the BER pathway, e.g. polymerase beta (POLβ), flap endonuclease 1 and nei endonuclease VIII-like 1 (*E. coli*) (NEIL1) (7–9). Mutations in the *WRN* gene are responsible for the Werner syndrome (WS), and both NBS and WS cells are characterized by a phenotype of genomic instability, putting these diseases to the group of chromosomal instability syndromes (9). As NBS1 and WRN interact with each other (6), common functions of these DNA repair proteins can be proposed. Therefore, we speculated about a function for NBS1 in the BER pathway as well. This hypothesis was further stimulated by studies analyzing the impact of NBS1 on neuronal cells. Neuronal cells are challenged by reactive oxygen species, generated in the brain due to its high oxygen consumption (10). Notably, the DNA BER pathway is essential for counteracting reactive oxygen species-induced oxidative damage and the maintenance of proper brain function and cell survival (10–13). In mice, a role for *NBS1* for the proliferation of granule cell progenitors and the avoidance of apoptosis of post-mitotic neurons in the cerebellum has been demonstrated (14). Furthermore, the NBS1 protein concentration seems to be enhanced in human Purkinje neurons, but decreased in neurons of Alzheimer's disease brains (15,16). Most interestingly, enhanced levels of oxidative base damage (10) and a reduced BER capacity of Alzheimer's disease brains (17) were recently reported, further motivating the theory that NBS1 contributes to the BER pathway.

The BER pathway consists of two subpathways, distinguished by the number of nucleotides that are incorporated during repair into the DNA molecule after removal of the damage. During single-patch repair, only one single nucleotide is built into the DNA and during long-patch repair, more than one nucleotide is incorporated into the molecule. Both subpathways of BER are initiated by the removal of the damaged base by glycosylases. Then, a nick is introduced at the apurinic or apyrimidic (AP) site. Cleaving at the AP sites can occur by different mechanisms and further enzymatic activities may be necessary to generate a 3′-OH group and a 5′-phosphate group to enable DNA synthesis and ligation (18). Thus, BER events are associated with the occurrence of single-strand breaks (SSBs) at the AP sites. SSBs trigger poly-(adenosine diphosphate-ribose)-polymerase-1 (PARP1) activity and poly-(adenosine diphosphate-ribose) (PAR) chains are synthesized under the consumption of nicotinamide adenine dinucleotide $(NAD)^+$ (19,20).

To analyze the importance of NBS1 for BER, we used RNA interference (RNAi) to downregulate *NBS1* expression in human *hTERT1*-immortalized retinal pigment epithelial (RPE) cells. We show for the first time that *NBS1* is indeed involved in the repair of base damage. NBS1-depleted cells are characterized by impaired PARP1 activation, resulting in reduced NAD^+ depletion and reduced PAR foci formation. Decreased BER capacity in extracts of *NBS1* downregulated cells was observed in an *in vitro* assay, affecting the long-patch as well as the short-patch subpathways. Moreover, BER capacity was found to be reduced in extracts from NBS patient cell lines compared with that from of consanguineous control cell lines.

Thus for the first time, our results identify a new function for NBS1 in the repair of DNA base damage by the BER pathway.

Abbreviations: AP, apurinic or apyrimidic; BER, base excision repair; ds, double stranded; DSB, double-strand break; EDTA, ethylenediaminetetraacetic acid; MMS, methyl methanesulfonate; MRN, MRE11/RAD50/NBS1; NAD, nicotinamide adenine dinucleotide; NBS, Nijmegen breakage syndrome; PAR, poly-(adenosine diphosphate-ribose); PARP1, poly-(adenosine diphosphate-ribose)-polymerase-1; PBS, phosphate-buffered saline; POLβ, polymerase beta; 8-oxoG, 8-oxo-7,8-dihydroguanine; RNAi, RNA interference; RPE, retinal pigment epithelial; siRNA, short interfering RNA; SSB, single-strand break; WS, Werner syndrome.

Materials and methods

Cell culture

The *hTERT1*-immortalized human RPE cell line was grown in Dulbecco's modified Eagle's medium/F12 (Gibco BRL Life Technologies, Karlsruhe, Germany) containing 2.5 mM L-glutamine, 10% fetal calf serum (PAA Laboratories, Pasching, Austria), 0.25% sodium bicarbonate supplemented with penicillin–streptomycin (10 IU/ml, Invitrogen, Karlsruhe, Germany) at 37°C in a humidified atmosphere containing 5% CO_2. Additionally, an $NBS1^{-/-}$ patient cell line and a consanguineous $NBS1^{+/-}$ cell line were used. These lymphoblastoid cell lines were kindly provided by Prof. Martin Digweed, Charité, Institute of Human Genetics, Berlin. They were propagated in RPMI 1640 medium (PAA), supplemented with 15% fetal calf serum (PAA) and penicillin–streptomycin (10 I.U./ml, Invitrogen) and incubated at 37°C in a humidified atmosphere containing 5% CO_2.

Cell transfection with siRNA

The day before transfection, $\sim 8 \times 10^4$ cells were seeded into a 60 mm diameter culture plate containing 5 ml Dulbecco's modified Eagle's medium/F12 medium. The next day, cells were either transfected with 10 nM control

(scrambled) short interfering RNA (siRNA) or with siRNA targeted against *NBS1* (UUCUCCGAACGUGUCACGUTT/CGGAUGAUGUGGCCAUAGAAGA) (Ambion, Darmstadt, Germany) using the siLentFect™ Lipid Reagent (Bio-Rad, Munich, Germany) according to the manufacture's instructions.

Cell survival assay after H_2O_2, respectively methyl methanesulfonate treatment

RPE cells were transfected with control siRNA or with siRNA targeted against *NBS1*. Twenty-four hours after transfection, the cells were seeded at an appropriate amount in 60 mm dishes. The cells were exposed to various concentrations of H_2O_2 (0–200 μM, Sigma, Munich, Germany) or methyl methanesulfonate (MMS) (0–1 mM, Sigma). In case of MMS treatment, medium was replaced by fresh medium after a treatment time of 2 h. After incubation for 7–10 days, any colonies were counted. Relative survival is given as the quotient of the plating efficiency of treated cells and untreated cells. Standard deviation was calculated from three independent experiments.

Relative survival of H_2O_2 treatment (0–80 μM) or MMS treatment (0–200 μM) of the patient cell lines is given as the quotient of the cell titer of a treated culture and that of an untreated one, 5 days after adding H_2O_2 to the medium. For MMS treatment, cells were pelleted by centrifugation and resuspended in fresh medium 2 h after treatment. Data represent mean ± SD for three independent experiments.

NAD^+ depletion assay

Forty-eight hours after transfection with control siRNA or siRNA targeted against *NBS1*, the cells were exposed to various concentrations of H_2O_2 (0–3 mM) or MMS (0–2 mM). For inhibition of PARP1 activity, cells were treated with 10 mM 3-aminobenzamide (Sigma) 45 min before treatment with H_2O_2 or MMS treatment. Two hours after H_2O_2 or MMS treatment, the cells were washed with phosphate-buffered saline (PBS), lysed with 0.1 M potassium phosphate buffer, pH 7.4/3% trichloroacetic acid and scraped off. The cell extracts were incubated 30 min on ice and then centrifuged for 5 min at high speed (>10 000*g*). The supernatant was neutralized with 0.8 M KOH/0.2 M Tris–HCl (200 μl/1 ml supernatant) and NAD^+ was quantified with slight modifications as described (21). A total of 0.9 ml thiazolyl blue tetrazolium bromide-mix [500 μM thiazolyl blue tetrazolium bromide (Sigma), 266 μM phenazine methosulfate (Sigma), 560 mM ethanol (Merck, Darmstadt, Germany), 18 units alcohol dehydrogenase (Sigma) in 100 mM potassium phosphate buffer, pH 7.4] was added to 0.2 ml neutralized supernatant and the reaction was incubated for 15 min at 30°C in the dark. Subsequently, the absorption was measured at 570 nm and NAD^+ amounts relative to amounts of extracts of untreated cells were calculated. Significances of relative differences of NAD amounts were analyzed by Student's *t*-test. The linearity of the reaction was controlled by calibrating with different amounts of NAD^+ (Sigma) as a standard. The remaining protein pellet was used for the control of the knockdown by western blot analysis. The pellet was heated with 200 μl Laemmli buffer (240 mM Tris–HCl, pH 6.8; 8% sodium dodecyl sulfate; 0.08% bromphenol blue; 40% glycerol; 20% 2-mercaptoethanol) for 10 min at 95°C and subjected to sodium dodecyl sulfate gel electrophoresis.

Detection of PAR formation

RPE cells were seeded onto glass slides and transfected with control siRNA or siRNA targeted against *NBS1*. Forty-eight hours after transfection, the cells were treated with H_2O_2 (0–3 mM) for 10 min at 37°C. Immunofluorescence analysis of PAR polymer formation was performed as described with slight modifications (22). The slides were washed three times with ice-chilled PBS, fixed with methanol:acetic acid (4:1, vol/vol) for 5 min at room temperature and washed again three times with ice-chilled PBS/0.1% Tween for 5 min. The incubation with the primary antibody was carried out overnight at 4°C with the polyclonal anti-PAR antibody (Alexis, Lörrach, Germany, 96-10-04) diluted 1:500 in PBS/0.1% Tween (vol/vol)/0.1% non-fat dry milk. After three washes with PBS/0.1% Tween for 5 min at room temperature, the slides were incubated for 2 h at room temperature with the 1:200 diluted goat anti-rabbit secondary antibody conjugated with Alexa Fluor 488 (Molecular Probes, Darmstadt, Germany, A11008). The slides were washed with PBS for 5 min and then the DNA was stained with Hoechst33342 (Sigma) for 2 min. After washing twice with PBS for 2 min, the slides were mounted with Vectashield (Vectashield Laboratories, Peterborough, England). Images were obtained using an LSM 510 NLO confocal laser scanning microscope (Carl Zeiss, Jena, Germany) and processed using LSM5 image software.

Protein analysis

To analyze protein expression by western blot analysis, cells were lysed with cell lysis buffer (Triton X-100, 1%; Tris–HCl, 25 mM, pH 7.4; NaCl, 120 mM supplemented with standard protease inhibitors). Western blot analysis was accomplished according to standard procedures using enhanced chemiluminescence detection (Amersham, Munich, Germany). For detection of NBS1 protein expression, the anti-NBS1 primary antibody from BioMol (Hamburg, Germany) (1D7) was used.

In vitro BER assay

Cell extract preparation (48 h after transfection) and the *in vitro* BER assay were performed as described (7). Briefly, the cells were resuspended in buffer I [10 mM Tris–HCl, pH 7.8; 200 mM KCl; protease inhibitor cocktail (Sigma)]. After adding an equal volume of buffer II [10 mM Tris–HCl, pH 7.8; 200 mM KCl; 2 mM ethylenediaminetetraacetic acid (EDTA); 40% glycerol; 0.2% Nonidet P-40; 2 mM dithiothreitol; protease inhibitor cocktail (Sigma)], the suspension was rotated for 1 h at 4°C and then centrifuged at 14 000 r.p.m. at 4°C for 30 min. The protein concentrations of the extracts were determined according to Bradford with bovine serum albumin as a standard.

Two different double-stranded (ds) DNA oligonucleotide substrates (generated by annealing BER1 and BER2 oligonucleotides) were used to determine repair capacity: one substrate contains a uracil at position 15 (BER1 5′-GCCCTGCAGGTCGAUTCTAGAGGATCCCCGGGTAC-3′ and BER2 5′-GTACCCGGGGATCCTCTAGAGTCGACCTGCAGGGC-3′) and the other contains an 8-oxo-7,8-dihydroguanine (8-oxoG) (marked as X) at this position (8-oxoG 5′-GCCCTGCAGGTCGAXTCTAGAGGATCCCCGGGTAC-3′ and BER2 5′-GTACCCGGGGATCCTCTAGAGTCGACCTGCAGGGC-3′). For generating the error-free control ds oligonucleotide, BER2 was annealed with BER0 (5′-GCCCTGCAGGTCGACTCTAGAGGATCCCCGGGTAC-3′).

The annealed DNA oligonucleotide substrates (concentration in reaction was 250 nM) were incubated with 3 μg extracted protein for 5 min at room temperature in BER reaction buffer [50 mM *N*-2-hydroxyethylpiperazine-*N*′-2-ethanesulfonic acid, pH 7.5; 0.5 mM EDTA; 2 mM dithiothreitol; 20 mM KCl; 4 mM adenosine triphosphate; 5 mM phosphocreatine; 0.5 mM NAD^+; 0.1 mM 3′-dideoxythymidine 5′-triphosphate; 20 μg/ml freshly added phosphocreatine kinase (Sigma)]. To initiate the repair reaction, 10 mM $MgCl_2$ and 2.2 μM [α-^{32}P]dCTP were added and the reaction tubes were incubated at 37°C. After the indicated time of incubation, the reaction was terminated by adding 5 mM EDTA and heating at 72°C for 5 min. To remove unincorporated [α-^{32}P]dCTP, the reaction was purified with G-25 Sephadex Columns for radiolabeled DNA purification (Roche, Penzberg, Germany) according to the manufacturer's instructions. An equal volume of DNA loading dye (95% formamide, 20 mM EDTA, 0.02% bromphenol blue, 0.02% xylene cyanol) was added and the products were denatured at 72°C for 2 min. The separation of the reaction products was done by gel electrophoresis (18% acrylamide, 8 M urea, 89 mM Tris–HCl (pH 8.8), 89 mM boric acid, 2 mM EDTA) and the reaction products were visualized by autoradiography and quantified by digital imaging (TotalLab, Amersham, UK).

Incision assay

To analyze incision capacity of the cell extracts, 10 μg protein of the cell extracts prepared for the BER assays was dissolved in reaction buffer (70 mM *N*-2-hydroxyethylpiperazine-*N*′-2-ethanesulfonic acid/KOH, pH 7.8; 10 mM dithiothreitol; 3 mM $MgCl_2$; 1 mM EDTA). Reactions were started by adding 2 pmol of ds uracil-containing oligonucleotides (see *in vitro* BER assay). To enable detection of reaction products after denaturing gel electrophoresis by autoradiography, the oligonucleotide-containing uracil was 5′-^{32}P labeled. Reactions were performed in a total volume of 10 μl at 32°C for 0, 5 or 10 min. Then, 100 μl stop solution (0.2% sodium dodecyl sulfate, 0.1 mg/ml Proteinase K) was added and the reactions were incubated at 60°C for 15 min. Reaction products were purified by phenol–chloroform extraction followed by ethanol precipitation. The dried reaction products were dissolved in 1:2 diluted DNA loading dye (see *in vitro* BER assay) and subjected to gel electrophoresis as described above. As a positive control, the reaction was performed by adding 1 U of uracil DNA glycosylase (New England Biolabs, Ipswich, USA) instead of protein extracts to the substrate. Subsequently, the phosphodiester bond at the AP site was hydrolyzed by adding NaOH to a total concentration of 150 mM and heating the reaction at 72°C for 20 min.

Results

NBS1-depleted cells show an increased sensitivity to DNA base-damaging agents

RNAi technology was used to repress endogenous *NBS1* levels in human RPE cells, allowing the comparative analysis of downregulated cells and appropriate control downregulated cells with an identical genomic background. This approach enabled us to study NBS1 functions that may not be observable in patient cell lines because the expressed NBS1 mutant proteins in these cells may have a residual activity (23). To determine sensitivity to DNA base damage, we performed H_2O_2 or MMS treatment of cells transfected with control siRNA or with *NBS1* siRNA. Three days after transfection,

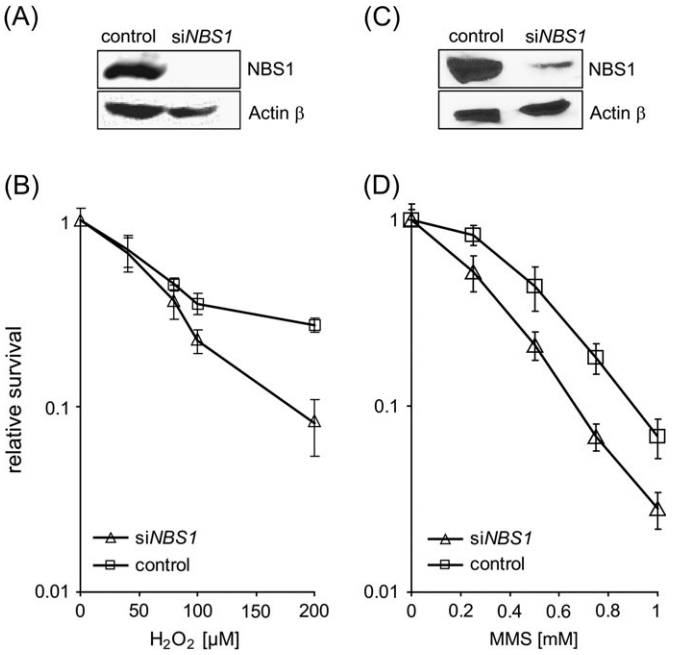

Fig. 1. *NBS1* is important for survival upon H_2O_2 or MMS treatment. (**A**) *NBS1* expression was downregulated by RNAi and protein expression levels were analyzed by western blotting 48 h after transfection. (**B**) Cell survival ± SD (three experiments) was analyzed by colony forming after treatment of control and *NBS1* downregulated cells with 0, 100, 200 or 300 μM H_2O_2. (**C**) For determination of survival upon MMS treatment, cells were again downregulated for NBS1 expression by RNAi and (**D**) cell survival was analyzed for 0, 250, 500, 750 or 1000 μM MMS.

knockdown efficiency for NBS1 was controlled by western blotting (Figure 1A and C). Relative cell survival was calculated by using a colony formation assay for H_2O_2- or MMS-treated cells. Cells downregulated for *NBS1* expression were more sensitive to H_2O_2 or MMS treatment as compared with control downregulated cells (Figure 1B and D). Since H_2O_2 and MMS both are DNA base-damaging agents, we proposed that reduced cell survival after knockdown of *NBS1* expression might be due to a reduced repair capacity for base damages.

NBS1 is necessary for full activation of PARP1 upon DNA base damage

To further elucidate this assumption, the following experiments were designed. *NBS1* expression was downregulated and cells were challenged with H_2O_2 or MMS treatment 2 days after transfection. Cell extracts were prepared to control knockdown efficiency (Figure 2A and C). Simultaneously, protein-free extracts were prepared from these cells to determine the relative NAD^+ amount normalized to that in extracts of untreated cells. NAD^+ depletion represents PARP1 activity, as NAD^+ is used by this enzyme to generate PAR chains after its activation by the SSBs that occur during BER (18,22,24). Knockdown of *NBS1* expression led to a reduced NAD^+ depletion compared with control downregulated cells (Figure 2B and D). The downregulation of *NBS1* led to a 2-fold decreased NAD^+ depletion after H_2O_2 or MMS treatment compared with control downregulated cells (2 or 3 mM H_2O_2/respectively 1 or 2 mM MMS). PARP1 dependency of the measured NAD^+ depletion after genotoxic treatment was confirmed by inhibiting PARP1 activity *in vivo* by pretreatment of the cells with 10 mM 3-aminobenzamide before adding of H_2O_2 or MMS. Under PARP1 inhibition, only a slight depletion of NAD^+ could be measured, demonstrating that the observed NAD^+ depletion is the result of PARP1 activity. These findings raise the possibility that H_2O_2- and MMS-induced PARP1 activity is decreased in the absence of NBS1. To substantiate this finding, we performed an immunofluorescence experiment to determine PAR as the product of the PARP1-catalyzed reaction. Control-transfected cells showed an inducible PAR formation with the strongest signal evident at 3 mM H_2O_2. Cells that were transfected with siRNA against *NBS1* showed severely decreased PAR formation. Significantly, PAR formation failed to increase with increasing H_2O_2 concentrations. Furthermore, increased levels of PAR formation were observed in non-treated *NBS1* downregulated cells as compared with the non-treated control downregulated cells (Figure 2E).

Summarizing these data, we conclude that *NBS1* downregulated cells are defective in PARP1 activation after inducing base damage by H_2O_2 or MMS treatment, which strongly suggests an influence of *NBS1* on BER.

BER capacity is reduced in extracts of NBS1 downregulated cells

In order to confirm that NBS1 is biochemically involved in the repair of DNA base damage, we performed *in vitro* BER assays according to Harrigan *et al.* (7) (Figure 3A). Repair of a 35 bp long duplex substrate containing at position 15 a single base triggering BER was analyzed. For this study, uracil or 8-oxoG was used as bases and [^{32}P]dCTP to label the repair products. In order to analyze products that were generated by long-patch BER as well as by short-patch BER, a 2′,3′-dideoxythymidine 5′-triphosphate stop nucleotide was added to the reaction. During the repair process, a [^{32}P]CMP nucleotide substitutes the nucleotide at position 15. If a ligation reaction takes place without any further reactions, a 35 bp long short-patch product is generated. For the long-patch repair pathway, additional DNA synthesis is required. Based on the designed sequence of the ds oligonucleotide and on the usage of ddTTP, 2′,3′-dideoxythymidine 5′-monophosphate is incorporated next to the incorporated [^{32}P]CMP and further strand elongation is blocked. Thus, a 16 bp long repair product is formed. Notably, in both repair pathways, a 15 bp long intermediate reaction product is generated with an unpredictable fate to be transformed to a 35 bp long short-patch repair product or to a 16 bp long long-patch repair product. Incorporation of the labeled nucleotide depends on the occurrence of uracil or 8-oxoG in the ds oligonucleotide substrate. No repair products were detected when using an error-free control ds oligonucleotide (Figure 3B). Experiments were done with four independently prepared sets of extracts of *NBS1* downregulated and of control downregulated cells. First, repair of the uracil-containing substrate was analyzed. Figure 3D shows a reduced BER repair capacity of extracts that were prepared from *NBS1* downregulated cells (efficiency of downregulation is shown in Figure 3C) in comparison with extracts that were produced from control downregulated cells for repairing the ds substrate containing uracil via both subpathways of BER. In Figure 3E, the average relative repair activity of the four extracts of *NBS1* downregulated cells compared with that of extracts of control downregulated cells is plotted for the long-patch and for the short-patch subpathways. For the long-patch subpathway, we find a 2.6 ± 0.4-fold decrease of repair capacity in extracts of *NBS1* downregulated cells, averaging over all time points where a repair product is visible in the assay with extracts of *NBS1* downregulated cells and of control downregulated cells, and a 2.1 ± 0.3-fold decrease of repair activity for the short-patch subpathway. To analyze if efficiency of base recognition or of incision of the DNA backbone at the AP site is influenced by NBS1, we performed an incision assay for the uracil-containing substrate (Figure 3F). No significant influence of the NBS1 status on these steps of BER could be detected. To examine if the observed defect of both subpathways of BER is specific for uracil, BER capacity was analyzed for repairing a substrate containing 8-oxoG instead of uracil. Again, impaired repair capacity of the extracts generated from *NBS1* downregulated cells was observed and again, both subpathways were affected (Figure 3G). Long-patch repair capacities were decreased by a factor of 1.7 ± 0.2 and short-patch capacities by a factor of 2.1 in extracts of *NBS1* downregulated cells (Figure 3H).

These results establish that NBS1 is important for the BER pathway, as *in vitro* BER of both substrates (uracil- and 8-oxoG-ds -oligonucleotides) is influenced by this protein, whereby the base recognition and incision steps are not affected.

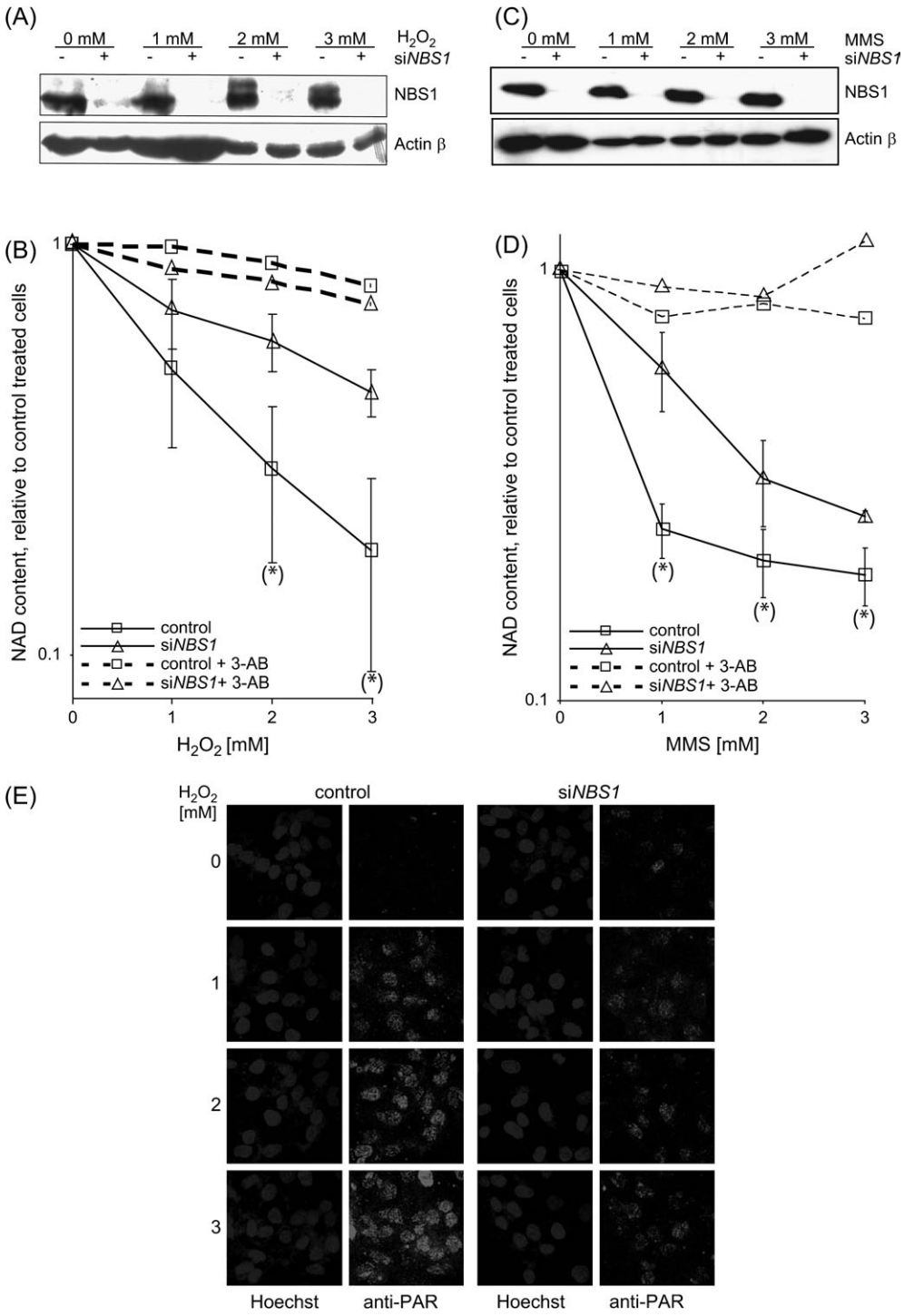

Fig. 2. PARP1 activation after base damage requires *NBS1*. (**A**) Efficiency of *NBS1* knockdown (+si*NBS1*) was controlled by western blotting 48 h after transfection. Equal gel loading was controlled by detection of actin β. One representative blot is shown for the three experiments. (**B**) NAD^+ depletion assay after H_2O_2 treatment of *NBS1* downregulated (si*NBS1*) or control downregulated cells with or without addition of 3-aminobenzamide (3-AB). Mean values of three independent experiments are shown ± SD. Asterisks below the data points indicate significant differences ($P < 0.05$). Only representative values of one experiment are shown for the 3-AB-treated cells. (**C** and **D**) Results for MMS treatment are shown as in (A and B). Data shown here summarize the results of four independent experiments. (**E**) Formation of PAR 10 min after treatment with 0, 1, 2 or 3 mM H_2O_2 was analyzed by immunofluorescence microscopy in *NBS1* downregulated (si*NBS1*) and control downregulated cells. Nuclei were stained with Hoechst33342. One of two independent experiments is shown.

Validation of the results with NBS patient cell lines

To strengthen our findings that NBS1 activates BER and that the described results are not an artifact of the RNAi technology, two approaches were repeated with an $NBS1^{-/-}$ patient cell line in comparison with a consanguineous $NBS1^{+/-}$ cell line. We could show that after treatment with H_2O_2 or MMS, the survival rate is influenced by the *NBS1* status. As the lymphoblastoid cell lines are more sensitive to H_2O_2 and MMS treatment compared with the *hTERT1*-immortalized RPE cell line, lower concentrations of H_2O_2 and MMS were used and $NBS1^{-/-}$ cells were more sensitive to these treatments as compared

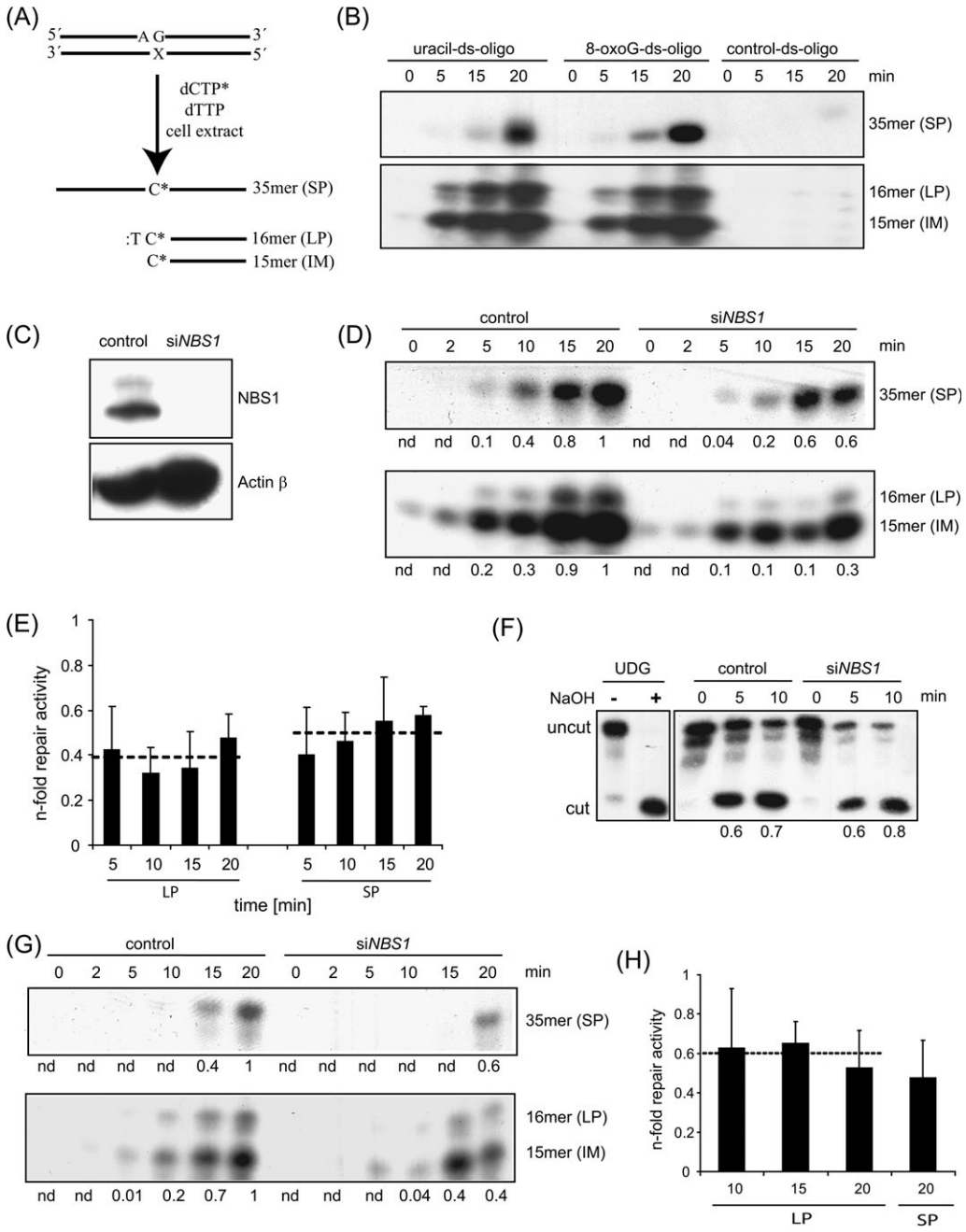

Fig. 3. *In vitro* BER capacity after knockdown of *NBS1* expression. (**A**) Labeled repair products generated by BER activity of the cell extracts. The short-patch product (SP) is detected as a 35 nucleotide (nt) long oligonucleotide, the size of the long-patch product (LP) is 16 nt. The intermediate product (IM) consists of 15 nt. Refer to text for further explanation. (**B**) Generation of repair products depend on the occurrence of a damaged base in the substrate. Repair capacity of cell extracts obtained from control downregulated cells was compared with the uracil-containing ds oligonucleotide, the 8oxoG-ds-oligonucleotide and for the error-free ds oligonucleotide. No repair products were detected for the error-free ds oligonucleotide. (**C**) Western blot analysis for NBS1 expression of one representative cell extract used for the *in vitro* BER assay. (**D**) Repair capacity for the repair of uracil-containing ds oligonucleotide of an extract of control downregulated cells and of *NBS1* downregulated cells (si*NBS1*). The numbers below the images indicate the relative band intensity of the corresponding band (for the SP or LP product) relative to the strongest band in that line. (**E**) Relative repair activities (mean ± SD) of extracts of *NBS1* downregulated cells as compared with extracts of control downregulated cells for the four independently prepared sets of cell extracts are shown. Only time points at which a repair product was visible in the assay with the extracts of *NBS1* downregulated cells and control downregulated cells were considered for the calculation. The dashed line indicates the average relative repair activity observed over all time points and all sets of extracts. LP and SP refer to the long-patch or short-patch repair pathway, respectively. (**F**) Incision assay for the uracil-containing ds oligonucleotide. Stability of the phosphodiester bond at the AP site was proven by using the uracil DNA glycosylase-treated substrate as control. Here, the effective generation of an AP site by uracil DNA glycosylase treatment was demonstrated by hydrolyzing the phosphodiester bond under alkaline conditions (+NaOH, left part of image). Generation of an AP site and incision activity of the extract was monitored through the appearance of a cut product of the repair substrate. Numbers below the lane indicate the ratio of the intensity of the band corresponding to the cut product to the sum of the intensities of the bands of the cut product and the uncut substrate. (**G** and **H**) like (D and E), but for the repair of an 8-oxoG containing ds oligonucleotide.

with *NBS1*$^{+/-}$ cells (Figure 4A and B). More importantly, the BER repair deficiency could be proven in extracts of *NBS1*$^{-/-}$ cells by the *in vitro* BER assay. Comparable with the results obtained with *NBS1* downregulated RPE cell extracts, an effect of NBS1 on both subpathways of BER was obtained, independently of the type of base damage that was repaired by the cell extract (Figure 4C and D).

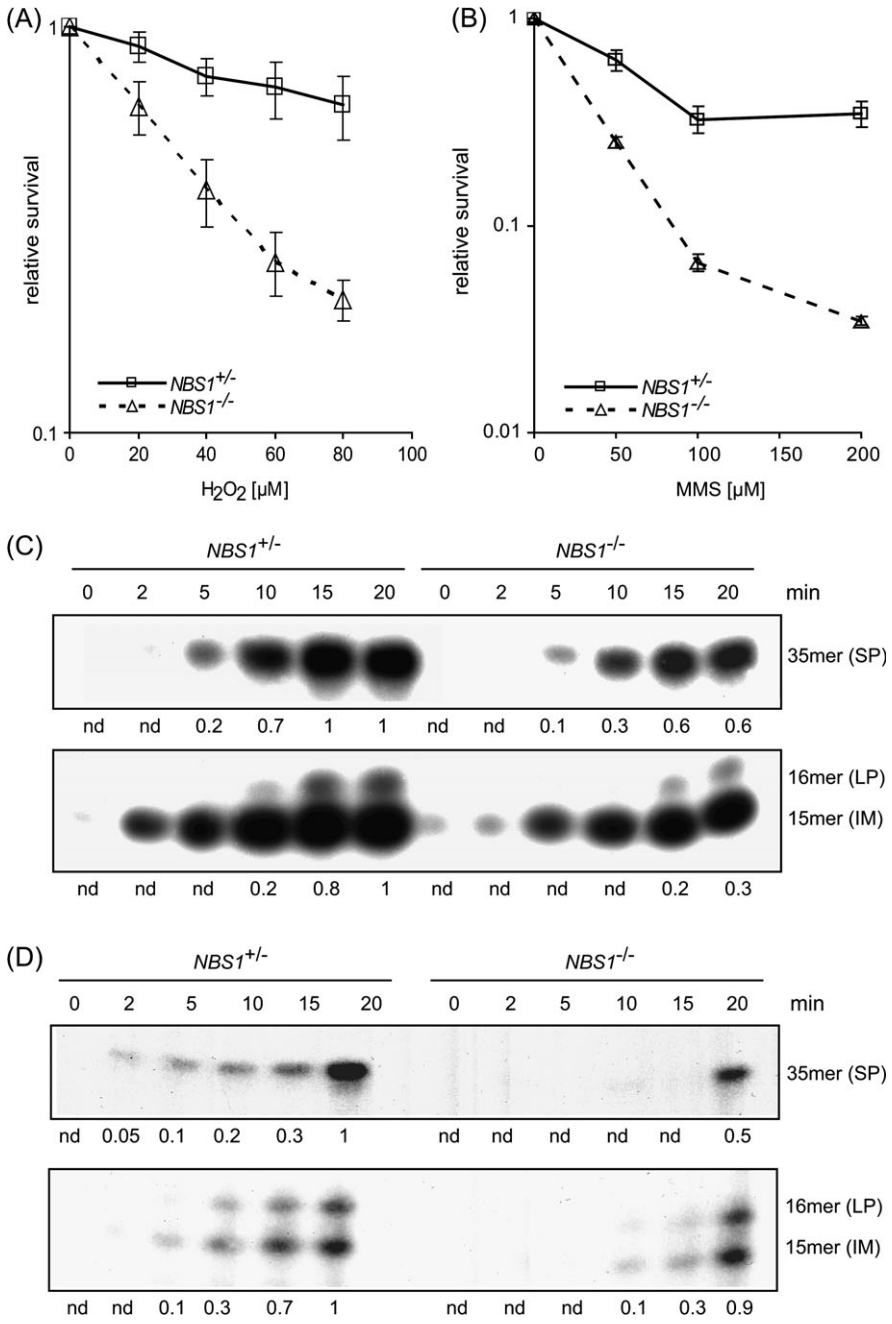

Fig. 4. Analysis of BER capacity in an *NBS1*$^{-/-}$ patient cell line. (**A**) Relative survival after genotoxic stress induced by H_2O_2 was analyzed by determining proliferation after H_2O_2 treatment with a concentration of 20, 40, 60 or 80 μM or (**B**) after MMS treatment with a concentration of 0, 50, 100 or 200 μM ± SD (three experiments). (**C**) BER capacity was determined by using the *in vitro* BER assay with a uracil-containing ds oligonucleotide or (**D**) with one containing 8-oxoG. The numbers below the images indicate the band intensities of the corresponding bands (for the SP and LP products) relative to the strongest band in the line.

Obviously, the stimulatory effect of NBS1 on BER could also be shown using material of an NBS patient cell line and is not only seen in cells that were NBS1-depleted by using RNAi.

Discussion

We demonstrate dependence of full active BER upon functional NBS1. The role of NBS1 for the BER pathway is reflected by the decreased survival rate of NBS1-depleted cells after genotoxic treatment with DNA base-damaging agents. In this study, DNA base damage was induced by H_2O_2, which is responsible for oxidative base damage, such as 8-oxoG, probably in concert with Fenton-type reactions (25,26), or MMS that is a potent inducer of mainly 7-methylguanine (27). One hallmark of *NBS1*-defective cells is their enhanced radiosensitivity, which has been linked to an impaired signaling or processing of DSBs (28) or enhanced radiation-induced apoptosis (29). Notably, ionizing radiation is a potent inducer of reactive oxygen species, especially together with oxygen (30), resulting in oxidative base damage in addition to DSBs. Thus, reduced survival of *NBS1*-defective cells after irradiation could also be caused in part by a decreased efficiency of the repair of base-damaged DNA as suggested by this paper for the first time.

As a first approach, consumption of NAD^+ by PARP1 was measured as an indicator for BER activity (21,22). We could demonstrate that PARP1-dependent depletion of the NAD^+ pool upon H_2O_2 or MMS treatment was reduced in cells that were downregulated for

the expression of *NBS1*. The reduced PARP1 activity in *NBS1* downregulated cells was confirmed by the detection of reduced PAR levels by immunofluorescence microscopy. Obviously, NBS1 is important for the full activation of PARP1 upon treatment with chemicals that induce SSBs. SSBs are generated either directly or indirectly by BER processes after or during the damaged base has been removed from the DNA backbone (31). The results of the *in vitro* BER assay substantiate a participation of NBS1 in BER. Both BER subpathways are influenced by NBS1 and the repair defect can be observed for each of two different repair substrates. However, no significant difference in the incision capacity of extracts of *NBS1* downregulated cells and control downregulated cells could be observed. The lack of influence of NBS1 on the incision step of BER confirms that base recognition and generation of SSBs are not affected by NBS1. Thus, we propose a role for NBS1 in BER for the recruitment of repair factors necessary for effective repair after an SSB has been introduced.

It has been demonstrated that the ability to synthesize PAR chains on other substrates than itself by PARP1 is stimulated by an interaction of this protein with WRN. Consequently, WS cells are impaired in PAR formation after H_2O_2 treatment (32) and this phenotype is mirrored in this study by the NBS1-depleted cells. As MRE11 has been described to interact with PARP1 at sites of DSBs (33), we propose that impaired PARP1 activation upon DNA damage might be the consequence of missing PARP1 stimulatory factors in NBS1-depleted cells, as in WS cells. The identities of these PARP1-activating partners are unknown, but it can be speculated that MRE11 or WRN is involved in this process, as they interact with PARP1 as well as with NBS1 as mentioned previously. Clearly, BER capacity of cell extracts is stimulated by NBS1, and PARP1 has been shown to stimulate this process *in vitro*, affecting both subpathways of BER (34). NBS1 stimulates both subpathways. Thus, NBS1 either stimulates BER by a mechanism that is common for both subpathways or activates it via different mechanisms. We suggest that NBS1 is essential for the generation of a functional PARP1-containing BER repair complex. This might especially explain the stimulatory effect of NBS1 on the long-patch subpathway, as the flap endonuclease 1 is stimulated by PARP1 (31). The impact of PARP1 on the short-patch subpathway is less clear. During the repair of SSBs via the SP subpathway, PARP1 and PAR recruit XRCC1 and eventually POLβ and LIG3 (35–37). In addition, LIG3 can also use PAR as a source of adenosine triphosphate (18).

At the moment, it can only be speculated how this PARP1-containing complex might affect BER. Since POLβ incorporates the first nucleotides into the repair substrates in both subpathways (18), we can assume that the regulation of the activity of POLβ is involved because impaired regulation of this polymerase can explain the observed repair defect in both subpathways. Indeed, this polymerase is regulated by and interacts with several proteins, like PARP1, WRN and apurinic-apyrimidinic endonuclease 1 (APE1) (38,39). Future *in vitro* studies analyzing the effect of purified NBS1 protein on the activation of PARP1 and the stimulation of POLβ will clarify the biochemical functions of NBS1 for BER. It is open, if NBS1 alone stimulates BER or the whole MRN complex. Preliminary experiments show impaired BER capacity of extracts of MRE11 or RAD50 downregulated cells (C.Kröger, personal communication). However, a depletion of RAD50 or MRE11 leads to a decrease in the cellular concentration of NBS1, whereas downregulation of *NBS1* gene expression does not affect RAD50 or MRE11 levels (40–42). Thus, full interpretation of these yet unpublished results requires more extensive research, if direct, NBS1-independent effects are to be analyzed.

Notably, the functions of NBS1 for the regulation of BER are supposed to be independent of ataxia telangiectasia mutated (ATM) as PARP1 activity and BER capacity is not impaired in ATM-defective cells (43,44), uncoupling our findings from the well-established model that NBS1 functions upstream and downstream of ATM (45,46). This report puts the DSB repair protein NBS1 into the context of an alternative DNA repair mechanism. Recently, an interaction of the MRN complex with the mismatch repair system has been published (47), illustrating the possibility of this complex to act on different DNA repair mechanisms beside DSB repair by homologous recombination or non-homologous end joining.

Funding

German Federal Ministry of Education and Research (02S8345).

Acknowledgements

The authors thank M.Digweed for the supply of the lymphoblastoid cell lines used for this study. We gratefully acknowledge the expert technical help from K.Winkler and thank M.Atkinson for critically reviewing the manuscript.

Conflict of Interest Statement: None declared.

References

1. Digweed,M. *et al*. (2004) Nijmegen breakage syndrome: clinical manifestation of defective response to DNA double-strand breaks. *DNA Repair (Amst.)*, **3**, 1207–1217.
2. The International Nijmegen Breakage Syndrome Study Group. (2000) Nijmegen breakage syndrome. *Arch. Dis. Child.*, **82**, 400–406.
3. Tauchi,H. *et al*. (2002) Nijmegen breakage syndrome gene, NBS1, and molecular links to factors for genome stability. *Oncogene*, **21**, 8967–8980.
4. Varon,R. *et al*. (1998) Nibrin, a novel DNA double-strand break repair protein, is mutated in Nijmegen breakage syndrome. *Cell*, **93**, 467–476.
5. Assenmacher,N. *et al*. (2004) MRE11/RAD50/NBS1: complex activities. *Chromosoma*, **113**, 157–166.
6. Cheng,W.H. *et al*. (2004) Linkage between Werner syndrome protein and the Mre11 complex via Nbs1. *J. Biol. Chem.*, **279**, 21169–21176.
7. Harrigan,J.A. *et al*. (2006) The Werner syndrome protein operates in base excision repair and cooperates with DNA polymerase beta. *Nucleic Acids Res.*, **34**, 745–754.
8. Das,A. *et al*. (2007) The human Werner syndrome protein stimulates repair of oxidative DNA base damage by the DNA glycosylase NEIL1. *J. Biol. Chem.*, **282**, 26591–26602.
9. Opresko,P.L. *et al*. (2003) Werner syndrome and the function of the Werner protein; what they can teach us about the molecular aging process. *Carcinogenesis*, **24**, 791–802.
10. Weissman,L. *et al*. (2007) DNA repair, mitochondria, and neurodegeneration. *Neuroscience*, **145**, 1318–1329.
11. Endres,M. *et al*. (2004) Increased postischemic brain injury in mice deficient in uracil-DNA glycosylase. *J. Clin. Invest.*, **113**, 1711–1721.
12. Kruman,I.I. *et al*. (2004) Suppression of uracil-DNA glycosylase induces neuronal apoptosis. *J. Biol. Chem.*, **279**, 43952–43960.
13. Vasko,M.R. *et al*. (2005) The multifunctional DNA repair/redox enzyme Ape1/Ref-1 promotes survival of neurons after oxidative stress. *DNA Repair (Amst.)*, **4**, 367–379.
14. Frappart,P.O. *et al*. (2005) An essential function for NBS1 in the prevention of ataxia and cerebellar defects. *Nat. Med.*, **11**, 538–544.
15. Gorodetsky,E. *et al*. (2007) ATM, the Mre11/Rad50/Nbs1 complex, and topoisomerase I are concentrated in the nucleus of Purkinje neurons in the juvenile human brain. *DNA Repair (Amst.)*, **6**, 1698–1707.
16. Jacobsen,E. *et al*. (2004) Deficiency of the Mre11 DNA repair complex in Alzheimer's disease brains. *Brain Res. Mol. Brain Res.*, **128**, 1–7.
17. Weissman,L. *et al*. (2007) Defective DNA base excision repair in brain from individuals with Alzheimer's disease and amnestic mild cognitive impairment. *Nucleic Acids Res.*, **35**, 5545–5555.
18. Fortini,P. *et al*. (2007) Base damage and single-strand break repair: mechanisms and functional significance of short- and long-patch repair subpathways. *DNA Repair (Amst.)*, **6**, 398–409.
19. Caldecott,K.W. (2003) XRCC1 and DNA strand break repair. *DNA Repair (Amst.)*, **2**, 955–969.
20. Petermann,E. *et al*. (2005) Importance of poly(ADP-ribose) polymerases in the regulation of DNA-dependent processes. *Cell. Mol. Life Sci.*, **62**, 731–738.
21. Matsumura,H. *et al*. (1980) Cycling assay for nicotinamide adenine dinucleotides. *Meth. Enzymol.*, **69**, 465–470.
22. Dantzer,F. *et al*. (2006) Poly(ADP-ribose) polymerase-1 activation during DNA damage and repair. *Meth. Enzymol.*, **409**, 493–510.
23. Maser,R.S. *et al*. (2001) An alternative mode of translation permits production of a variant NBS1 protein from the common Nijmegen breakage syndrome allele. *Nat. Genet.*, **27**, 417–421.
24. Kim,M.Y. *et al*. (2005) Poly(ADP-ribosyl)ation by PARP-1: 'PAR-laying' NAD+ into a nuclear signal. *Genes Dev.*, **19**, 1951–1967.
25. Jena,N.R. *et al*. (2005) Mechanisms of formation of 8-oxoguanine due to reactions of one and two OH^* radicals and the H2O2 molecule with

guanine: a quantum computational study. *J. Phys. Chem. B*, **109**, 14205–14218.
26. Moriwaki,H. *et al*. (2008) Effects of mixing metal ions on oxidative DNA damage mediated by a Fenton-type reduction. *Toxicol. In Vitro.*, **22**, 36–44.
27. Beranek,D.T. (1990) Distribution of methyl and ethyl adducts following alkylation with monofunctional alkylating agents. *Mutat. Res.*, **231**, 11–30.
28. Kobayashi,J. *et al*. (2004) NBS1 and its functional role in the DNA damage response. *DNA Repair (Amst.)*, **3**, 855–861.
29. Sagan,D. *et al*. (2007) Enhanced CD95-mediated apoptosis contributes to radiation hypersensitivity of NBS lymphoblasts. *Apoptosis*, **12**, 753–767.
30. LaVerne,J.A. (2000) OH radicals and oxidizing products in the gamma radiolysis of water. *Radiat. Res.*, **153**, 196–200.
31. Caldecott,K.W. (2008) Single-strand break repair and genetic disease. *Nat. Rev. Genet.*, **9**, 619–631.
32. von Kobbe,C. *et al*. (2003) Central role for the Werner syndrome protein/poly(ADP-ribose) polymerase 1 complex in the poly(ADP-ribosyl)ation pathway after DNA damage. *Mol. Cell. Biol.*, **23**, 8601–8613.
33. Haince,J.F. *et al*. (2008) PARP1-dependent kinetics of recruitment of MRE11 and NBS1 proteins to multiple DNA damage sites. *J. Biol. Chem.*, **283**, 1197–1208.
34. Dantzer,F. *et al*. (2000) Base excision repair is impaired in mammalian cells lacking Poly(ADP-ribose) polymerase-1. *Biochemistry*, **39**, 7559–7569.
35. El-Khamisy,S.F. *et al*. (2003) A requirement for PARP-1 for the assembly or stability of XRCC1 nuclear foci at sites of oxidative DNA damage. *Nucleic Acids Res.*, **31**, 5526–5533.
36. Godon,C. *et al*. (2008) PARP inhibition versus PARP-1 silencing: different outcomes in terms of single-strand break repair and radiation susceptibility. *Nucleic Acids Res.*, **36**, 4454–4464.
37. Masson,M. *et al*. (1998) XRCC1 is specifically associated with poly(ADP-ribose) polymerase and negatively regulates its activity following DNA damage. *Mol. Cell. Biol.*, **18**, 3563–3571.
38. Confer,N.F. *et al*. (2004) Biochemical association of poly(ADP-ribose) polymerase-1 and its apoptotic peptide fragments with DNA polymerase beta. *Chem. Biodivers.*, **1**, 1476–1486.
39. Sukhanova,M.V. *et al*. (2005) Human base excision repair enzymes apurinic/apyrimidinic endonuclease1 (APE1), DNA polymerase beta and poly(ADP-ribose) polymerase 1: interplay between strand-displacement DNA synthesis and proofreading exonuclease activity. *Nucleic Acids Res.*, **33**, 1222–1229.
40. Hematulin,A. *et al*. (2008) NBS1 is required for IGF-1 induced cellular proliferation through the Ras/Raf/MEK/ERK cascade. *Cell. Signal.*, **20**, 2276–2285.
41. Stewart,G.S. *et al*. (1999) The DNA double-strand break repair gene hMRE11 is mutated in individuals with an ataxia-telangiectasia-like disorder. *Cell*, **99**, 577–587.
42. Zhong,H. *et al*. (2005) Rad50 depletion impacts upon ATR-dependent DNA damage responses. *Hum. Mol. Genet.*, **14**, 2685–2693.
43. Cappelli,E. *et al*. (2000) Efficient DNA base excision repair in ataxia telangiectasia cells. *Eur. J. Biochem.*, **267**, 6883–6887.
44. Dantzer,F. *et al*. (1999) Poly(ADP-ribose) polymerase activity is not affected in ataxia telangiectasia cells and knockout mice. *Carcinogenesis*, **20**, 177–180.
45. Lee,J.H. *et al*. (2004) Direct activation of the ATM protein kinase by the Mre11/Rad50/Nbs1 complex. *Science*, **304**, 93–96.
46. Shiloh,Y. (2003) ATM and related protein kinases: safeguarding genome integrity. *Nat. Rev. Cancer*, **3**, 155–168.
47. Mirzoeva,O.K. *et al*. (2006) The Mre11/Rad50/Nbs1 complex interacts with the mismatch repair system and contributes to temozolomide-induced G2 arrest and cytotoxicity. *Mol. Cancer Ther.*, **5**, 2757–2766.

Received August 31, 2008; revised November 25, 2008; accepted December 22, 2008